Enhancing the Stability of the Electron Density in Electrochemically Doped ZnO Quantum Dots

Gudjónsdóttir, Sólrún; Houtepen, Arjan; Koopman, Christel

DOI
10.1063/1.5124534

Publication date
2019

Document Version
Final published version

Published in
Journal of Chemical Physics

The Journal of Chemical Physics

Enhancing the stability of the electron density in electrochemically doped ZnO quantum dots

Cite as: J. Chem. Phys. **151**, 144708 (2019); https://doi.org/10.1063/1.5124534
Submitted: 15 August 2019 . Accepted: 25 September 2019 . Published Online: 11 October 2019

Solrun Gudjonsdottir, Christel Koopman, and Arjan J. Houtepen

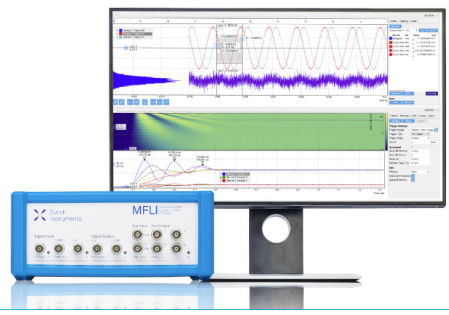

The Journal of Chemical Physics ARTICLE scitation.org/journal/jcp

Enhancing the stability of the electron density in electrochemically doped ZnO quantum dots

Cite as: J. Chem. Phys. 151, 144708 (2019); doi: 10.1063/1.5124534
Submitted: 15 August 2019 • Accepted: 25 September 2019 •
Published Online: 11 October 2019

Solrun Gudjonsdottir, Christel Koopman, and Arjan J. Houtepen[a)]

AFFILIATIONS

Chemical Engineering, Optoelectronic Materials, Delft University of Technology, Van der Maasweg 9, 2629 HZ Delft, The Netherlands

Note: This paper is part of the JCP Special Topic on Colloidal Quantum Dots.
[a)]A.J.Houtepen@tudelft.nl

ABSTRACT

Electronic doping of semiconductor nanomaterials can be efficiently achieved using electrochemistry. However, the injected charge carriers are usually not very stable. After disconnecting the cell that is used for electrochemical doping, the carrier density drops, typically in several minutes. While there are multiple possible causes for this, we demonstrate here using n-doped ZnO quantum-dot (QD) films of variable thickness that the dominant mechanism is reduction of solvent impurities by the injected electrons. We subsequently investigate two different ways to enhance the doping stability of ZnO QD films. The first method uses preemptive reduction of the solvent impurities; the second method involves a solid covering the QD film, which hinders impurity diffusion to the film. Both methods enhance the doping stability of the QD films greatly.

INTRODUCTION

Electrochemical doping provides a controlled way of changing the charge carrier density of semiconductor materials. So far, (spectro)-electrochemical measurements have been mainly used as an analytical tool[1–3] for a wide range of semiconductor materials,[4–8] but electrochemistry can also be a powerful method to permanently dope porous semiconductor films. In electrochemical doping, the semiconductor material is deposited on a working electrode (WE) and placed in an electrochemical cell. By changing the potential between the WE and a reference electrode (RE), electrons can be injected into or extracted from the semiconductor film. That is, the Fermi-level and the charge carrier density of the semiconductor film can be tuned by changing the potential.[2,9] The requirement for efficient electrochemical doping is that counterions, which compensate the charge of injected electrons/holes, can diffuse into the material and result in 3D charge compensation.

Electrochemical doping has predominantly been used for conducting polymers.[10] A notable example is that of the light emitting electrochemical cell, wherein a potential difference on a planar two-electrode electrochemical cell results in the *in situ* formation of a *p-i-n* junction that exhibits light emission in the *i* region.[11,12] Electrochemical doping has also been applied to films of semiconductor nanocrystals,[2,4,13–15] fullerenes,[16] and carbon nanotubes.[17]

However, stable electrochemical doping has not been achieved, as when the electrochemical cell is disconnected from the potentiostat, the injected charges spontaneously leave the semiconductor film.[2,9,12,18] The loss of injected charges can be caused by either electrochemical reactions of the material itself[2,19–21] or by solvent impurities.[22] It is known that impurities can affect doping stability greatly.[23,24] Gamelin *et al.* showed that by exposing *n*-doped nanocrystals to air or other appropriate oxidants, the injected charge was removed and the nanocrystals returned to their original oxidation state.[25,26] Additionally, solvent impurities do not only affect electrochemical doping of the material, but they can also induce a large variation in electrochemical measurements.[27–29] It is highly desirable to increase the stability of electrochemically injected charge carriers so that this technique could be used to prepare active and stable junctions in devices such as light emitting diodes.

Here, we investigate the electrochemical doping stability of ZnO quantum dots (QDs) in anhydrous acetonitrile solution dried

over an activated alumina column (Innovative Technology PureSolv Micro, water content around 5 ppm without 0.1M $LiClO_4$ and 11.8 ppm with 0.1M $LiClO_4$ measured by Karl Fischer titration), performed in a nitrogen filled glovebox (oxygen ≤0.1 ppm and moisture ≤0.5 ppm). Even under these conditions, it is observed that injected electrons gradually leave the conduction band of the QDs after disconnecting the electrochemical cell. We find that the apparent charge stability is a strong function of ZnO QD film thickness. This implies that solvent impurities, rather than electrochemical reactions in the ZnO QD films, are the dominant cause of the decay of the charge density.

Next, we sought methods to eliminate the effect of solvent impurities on the charge stability, by reducing any eventual impurity oxidant before electrochemical doping or by covering the film with a solid film of succinonitrile that prevents impurity diffusion. We show that by using either electrochemical or chemical reduction of the solvent impurities, the doping stability of the doped ZnO QD film increases immensely. When the electrolyte solvent is exposed to a reducing potential (−1.0 V vs Ag pseudoreference electrode), this results in an 18-fold increase in doping stability, as determined with Fermi-level stability measurements. Chemical reduction of the solvent impurities is achieved by addition of superhydride, $Li[Et_3BH]$. This greatly improves the doping stability of the ZnO QDs, by about a factor 100.

Both approaches are effective, but only for a limited time, as more oxidants will inevitably diffuse into the doped film. To prevent this, we have used succinonitrile as an alternative solvent with a melting point of 57 °C. After charging at 60 °C, the film is quickly removed from the solvent and treated in various ways. This leads to the quick solidification of the succinonitrile and the formation of a protective thin solid film around the doped ZnO QDs. In the best cases, the loss of injected charge density is around 4% after 2 h. These results demonstrate possible avenues for enhancing the stability of electrochemically injected charges in semiconductor films.

EXPERIMENTAL METHODS

Materials

Zinc acetate dihydrate [$Zn(CH_3COO)_2{\cdot}2H_2O$ reagent grade], potassium hydroxide (KOH pellets), Indium-doped Tin Oxide (ITO) substrates, lithium perchlorate ($LiClO_4$, 99.99%), ferrocene (Fc, 98%), anhydrous solvents [acetonitrile, 99.99%; tetrahydrofuran (THF), 99.9%; methanol, 99.8%; ethanol (max 0.01% H_2O); hexane, 95%], succinonitrile (99%), and superhydride (1M $Li[Et_3BH]$ in THF). All chemicals were purchased from Sigma Aldrich unless stated otherwise. Acetonitrile and THF were dried before use in an Innovative Technology PureSolv Micro column. All other chemicals were used as received.

ZnO QD synthesis and film preparation

The ZnO QDs were synthesized as previously described.[30] 3.425 mmol of zinc acetate dihydrate was combined with 50 ml ethanol in an Erlenmeyer flask at 60 °C. In the meantime, 6.25 mmol KOH was mixed with 5 ml methanol in a vial. When both mixtures were clear, the KOH mixture was added dropwise (approximately 1 drop per second) to the Erlenmeyer flask. After the addition of KOH, the heat source was removed after one additional minute. The ZnO QDs were purified by the addition of hexane and isolated by centrifugation at 2000 rpm for 1 min. The QDs were redissolved in ethanol and stored at −20 °C to avoid further growth by Ostwald ripening. The ZnO QDs were drop casted either on an ITO or on a home-made interdigitated gold electrode (IDE, supplementary material Fig. S1) and annealed at 60 °C for an hour. The diameter of synthesized QDs was calculated as 3.6 nm by using the empirical correlation from the work of Meulenkamp.[31]

Electrochemical measurements

All electrochemical measurements were performed in a N_2 filled glovebox with an Autolab PGSTAT128N potentiostat. A 3-electrode electrochemical cuvette cell was used, where the sample was deposited on the working electrode (WE). The WE was either an ITO or IDE and was immersed into 0.1M $LiClO_4$ acetonitrile or succinonitrile solution. The solution also contains an Ag wire as a pseudoreference electrode (PRE) and a Pt sheet as a counter electrode (CE). The PRE was calibrated with a ferrocene/ferrocenium couple, and its potential was found to be constant at −4.76 eV vs vacuum.

Cyclic voltammetry measurements (CVs)

Every CV was performed at 0.05 V/s. The measurements were performed between 0 V and −1.0 V and reversed.

Fermi-level stability measurements

Fermi-level stability measurements were performed after charge injection into the conduction band of the QDs took place. When the system had reached an equilibrium, the CE was disconnected from the RE and the WE. By doing so, no more electrons could be injected into the QDs. The change in potential between the WE and the RE was measured vs time. This potential is connected to the Fermi-level of the WE vs the Fermi-level of the RE. If electrons leave the conduction band of the QDs, the Fermi-level will drop, which leads to an increase in the measured potential.

Conductance measurements

Conductance measurements were performed on an IDE after electron injection into the conduction band of the QDs took place. When the system had reached an equilibrium, the potentiostat was disconnected and the conductance was measured with a Keithley 2400 source meter. After the sample is disconnected from the potentiostat, no electrons can be injected into the conduction band of the QDs. The source-drain potential difference used was 10 mV.

RESULTS AND DISCUSSIONS

Electrochemical doping of ZnO QD films

Figure 1(a) shows a cyclic voltammogram (CV) and the differential absorbance at the band edge (360 nm) for a ZnO QD film

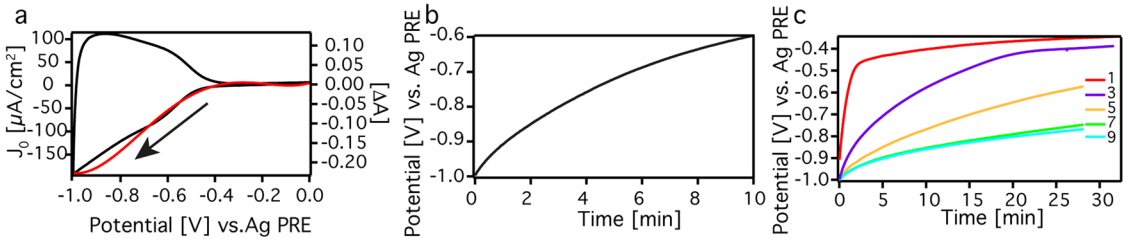

FIG. 1. Spectro-electrochemical measurements performed on ZnO QD films in 0.1M $LiClO_4$ acetonitrile solution. (a) CV (shown in black) measured at 0.05 V/s; the arrow indicates the scan direction. The graph includes the differential band edge absorbance, ΔA (shown in red). J_0 stands for the current density. The sample is made of 3 drop casting steps. (b) Fermi-level stability measurement of a ZnO QD film. Before the CE was disconnected, the potential was kept at −1.0 V until equilibrium was reached. When the injected electrons leave the QDs, the Fermi-level drops, which corresponds to an increase in potential. The sample is made of 3 drop casting steps. (c) Fermi-level stability measurement for ZnO QD films of different thicknesses. The films were made of 1, 3, 5, 7, and 9 drop casting steps of QD solution. Measured profilometry thicknesses are shown in supplementary material, Table S1. By increasing the film thickness, the doping stability increases.

in 0.1M $LiClO_4$ acetonitrile solution. The 2D plot of the differential absorbance is shown as Fig. S2 in the supplementary material. The scan starts at 0 V vs an Ag pseudoreference electrode (PRE), which corresponds to a Fermi level in the bandgap of the ZnO QD film. At around −0.5 V, the current becomes more negative and the band edge absorbance decreases due to state filling, which shows that electrons are injected into the conduction band of the QDs.[30] From the measured current, I, it is possible to calculate the total amount of injected (or extracted on the reverse scan) electrons with the following equation:

$$n_e = \sum \frac{(I * dE)}{v * e * V}, \tag{1}$$

where dE is the potential step (here 0.002 44 V), v is the scan rate (here 50 mV/s), e is the elementary charge, and V is the film volume. By the use of Eq. (1), we find that the charge density is increased to $2.24 * 10^{18}$ cm^{-3} at −1.0 V. The ratio between extracted and injected electrons is 0.856 for the measurement in Fig. 1(a). This means that almost 15% of the injected electrons are not extracted in the return scan. To investigate this loss of electrons in more detail, so-called Fermi-level stability measurements are performed [Fig. 1(a)]. In this experiment, the potential is changed to −1.0 V, at which point the counter electrode (CE) is disconnected and the potential of the working electrode (WE) vs the pseudoreference electrode (PRE) is recorded. If electrons leave the system, the potential returns to the original open circuit potential (V_{oc}, around 0 V). The same trend is also seen from the change in differential absorbance during the Fermi-level stability measurements (supplementary material, Fig. S3). Figure 1(b) shows that in only 10 min, the potential increases by about 0.4 V. From the not fully reversible CV and the Fermi-level stability measurement, it is clear that many injected electrons are lost.

As previously discussed,[32] we consider three possible reasons for electrons leaving the quantum dot film. First, electrochemical reactions can occur within the material itself.[2,33–35] For instance, surface Zn^{2+} ions on the QDs could potentially reduce to Zn^0.[36] Second, counter ions could move out of the film. Such counter ion movement is especially expected in devices where an electric field is present;[10] however, in the present experiments, such an electric field is not expected to be present. Third, solvent impurities such as water or molecular oxygen can react with injected electrons. Indeed, when similar measurements are performed outside of the glovebox, it leads to much less symmetric CVs (supplementary material, Fig. S4).

To test which mechanism is responsible for the observed spontaneous drop of the Fermi level, we performed measurements on films of varying thickness. Increasing the film thickness implies that, for a fixed amount of impurities, the relative change of the electron concentration in the ZnO QD film is smaller. Hence, if solvent impurities are responsible for the electron loss, then increasing the film thickness should improve the doping stability. However, if electrochemical reactions within the ZnO QDs are responsible, increasing the thickness will not help.

Fermi-level stability measurements were performed on ZnO QD films of different thicknesses in a fresh electrolyte solution of the same volume from the same batch of electrolyte solution [Fig. 1(c)]. The films were made by increasing the number of drop casted steps. To verify the increasing thickness, CVs and profilometer measurements were performed (supplementary material, Fig. S5 and Table S1). Figure 1(c) shows that increasing the film thickness indeed leads to a much slower drop of the Fermi level. As the films are highly porous and the solvent permeates throughout the film,[30] this shows that electron extraction is predominantly caused by impurities in the electrochemical environment.

To prevent impurities from oxidizing the QDs, it should be possible to reduce them before they react with injected electrons. One way of reducing the solvent impurities is by applying a negative potential to the solution before the measurements with the ZnO QD film, that is, by using a cathodic preconditioning. Figure 2(a) shows Fermi-level stability measurements before and after applying the cathodic preconditioning of −1.0 V to the electrolyte solution for 2 h. When applying the potential, a bare ITO is used to make sure that no changes occur to the ZnO QD film. Without cathodic preconditioning of the electrolyte solution, it takes 32 s to get a potential decay of 0.15 V, while the same change in potential takes 10 min after the solvent preconditioning. This can be seen, somewhat arbitrarily, as an 18-fold increase in doping stability. However, if the electrochemical cell is disconnected from the potentiostat for about 4 h between the measurements, the potential decay is again similar

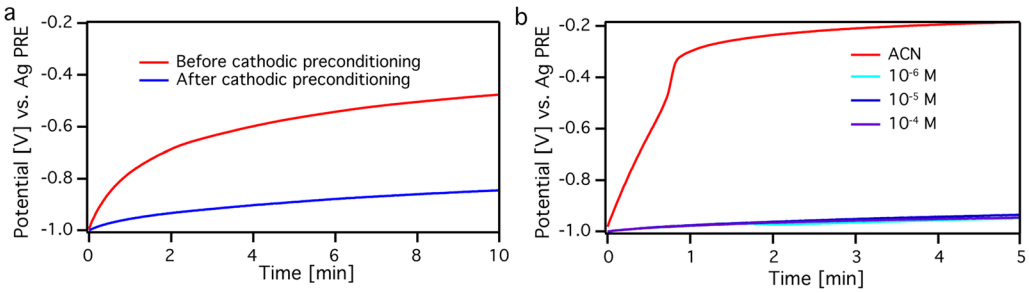

FIG. 2. Impurities are reduced in a 0.1M $LiClO_4$ acetonitrile (ACN) electrolyte solution. (a) Fermi-level stability measurements for a ZnO QD film on an ITO before and after a cathodic precondition of −1.0 V was applied to the electrolyte solution (with a bare ITO for 2 h). (b) Fermi-level stability measurements performed with different concentrations of $Li[Et_3BH]$ ranging from 10^{-6} to 10^{-4}M. By performing a cathodic preconditioning step or by adding superhydride to the solution, the doping stability increases greatly.

to original values (supplementary material, Fig. S6). We tentatively conclude that only a part of the solution is reduced during the treatment. We consider that reduced impurities may again be oxidized at the counter electrode, causing the electrolyte solution to reestablish equilibrium over a couple of hours.

A supposedly irreversible way[37] of reducing the impurity atoms is by using superhydride, $Li[Et_3BH]$.[25,26,37] Upon oxidizing, $Li[Et_3BH]$ decomposes into hydrogen gas and triethylborane; therefore, the reversed reaction does not take place at the same potential.[38,39] Figure 2(b) shows Fermi-level stability measurements for a ZnO QD film in 0.1M $LiClO_4$ acetonitrile solution with a concentration of $Li[Et_3BH]$ ranging from 10^{-6} to 10^{-4}M. Higher concentrations of superhydride caused sample instability for the ZnO QD film. Both the open circuit potential and the absorbance of the film were measured when the superhydride was added to the acetonitrile solution to make sure that the superhydride did not reduce the ZnO QDs. No bleach and no significant change in the open circuit potential were seen during the addition (see supplementary material, Table S2). For reference, a Fermi-level stability measurement was performed on the sample before the addition of the $Li[Et_3BH]$ to the acetonitrile solution. Adding a small amount of $Li[Et_3BH]$ greatly increases the doping stability. Before the addition of superhydride, it takes 3 s for the potential to reach a decay of 0.05 V, while it takes around 5 min after the addition of superhydride. As before, somewhat arbitrarily, this can be seen as a 100-fold increase in doping stability. Increasing the concentration from 10^{-6} to 10^{-4}M improves the stability only marginally.

To quantify the increased doping stability, CVs were performed at every concentration of added $Li[Et_3BH]$ (supplementary material, Fig. S7). From the CVs, the ratio between injected and extracted electrons is calculated and shown in Table I. Without superhydride, 89.8% of the injected electrons are extracted. This charging/discharging ratio increases to 98.7% for 10^{-4} M superhydride. Thus, $Li[Et_3BH]$ is able to reduce most solvent impurities, which leads to increased charge stability during CVs and Fermi-level stability measurements. However, a small amount of electrons is still lost. This might be due to internal electrochemical reactions of the ZnO QDs themselves or it is possible that residual oxygen or water, or perhaps other impurities, from the glovebox environment diffuses into the electrolyte, making it impossible to remove all impurities.

TABLE I. Ratio between extracted and injected electrons for the QD film measured in different concentrations of superhydride in acetonitrile.

	ACN	10^{-6}M	10^{-5}M	10^{-4}M
Ratio	0.898	0.978	0.941	0.987

In all experiments so far, the doped ZnO QD film remained submerged in the electrolyte solvent. This is necessary for the Fermi level stability measurements. However, since it appears that impurities in the solvent are dominant in the drop of the charge density, it would be interesting to see the charge stability in the absence of the electrolyte. To facilitate this, we have performed source-drain conductivity experiments vs time. A ZnO QD film on an interdigitated source-drain electrode is charged so that the conductance increases strongly. Subsequently, the CE is disconnected and the source drain conductance is measured with a Keithley 2400 source meter. This can also be done after the film is removed from the electrochemical cell and is no longer in contact with the electrolyte. A decrease in conductance means that the electron density decreases.

Four different conductance measurements were performed on the same ZnO QD film: in an acetonitrile solution, in an acetonitrile solution containing 10^{-3}M superhydride, on a dry film (after the film was taken out of the solution), and on a film dried in vacuum after charging but before the conductance measurements. As the conductance measurements are not started at exactly the same time after disconnecting the electrochemical cell, the initial conductance varies slightly. Therefore, the normalized results are shown in Fig. 3(a) (the original traces are in supplementary material, Fig. S8).

Clearly, the quickest decay of the conductance is observed for the film in acetonitrile solution. We note that the conductance in Fig. 3(a) drops more rapidly than the potential in Fig. 2 because the potential scales logarithmically with electron density (through the Nernst law), while the conductivity σ (and hence also the conductance) scales approximately linearly with the electron density

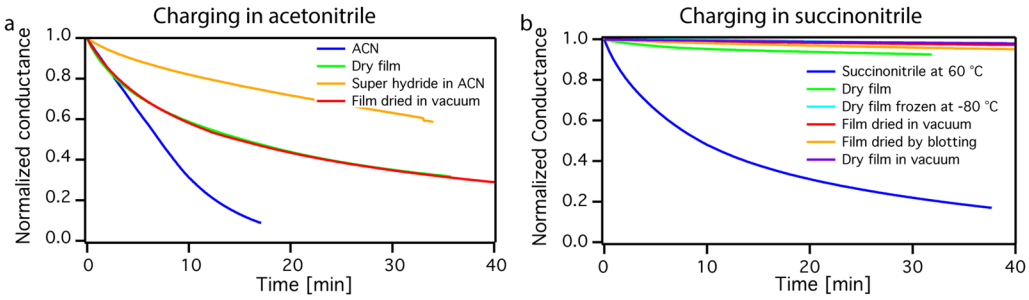

FIG. 3. Conductance measurements after charge injection for a ZnO QD film. (a) Measurements performed in 0.1M $LiClO_4$ acetonitrile solution (ACN) (blue), acetonitrile solution with the addition of superhydride (yellow), for a film taken out of the solution (dry film, green), and for a film dried in vacuum for 1 min (red). (b) Measurements performed in 0.1M $LiClO_4$ succinonitrile solution at 60 °C (blue), for a dry film (green), after the sample was blotted with a filter paper (yellow), after the sample was stored under vacuum for 1 min (red), after the sample was plunged into THF at −80 °C (cyan), and for a film in vacuum (purple).

(via $\sigma = ne\mu$, where n is the electron density, e is the electron charge, and μ is the electron mobility). As the mobility decreases rapidly with decreasing electrochemical potential in the bandgap,[30] the drop in conductivity is further enhanced.

Figure 3(a) shows that by taking the film out of the solution, the conductance decays more slowly. Additionally, the doping stability of the ZnO QD film does not increase by drying it in vacuum for a minute. Interestingly, the best stability is gained by measuring the conductance in an acetonitrile solution containing superhydride. This suggests that the superhydride treated acetonitrile solution contains less contaminants than the glovebox environment. This also implies that on longer time scales diffusion of impurities from the glovebox environment into the solution may cause the stability to decrease again. Therefore, it is important to avoid diffusion of impurities to the film altogether.

One way to reduce impurity diffusion is to cover the film with a solid protective layer. A convenient way to achieve this is by using an electrolyte solvent that is solid at room temperature. An example is succinonitrile, which is similar in electrochemical stability to acetonitrile but has a melting point of 57 °C. Therefore, we performed source-drain conductivity measurements on a ZnO QD film measured in 0.1M $LiClO_4$ succinonitrile solution. The film is charged at 60 °C, above the melting point of succinonitrile. After the film is charged at −1.0 V, the CE is disconnected and the film is taken out of the solution. As the sample cools to room temperature, the succinonitrile covering the film solidifies quickly and the source-drain conductance is measured. A CV for a ZnO QD film measured in 0.1M $LiClO_4$ in succinonitrile at 70 °C is shown in supplementary material, Fig. S9.

Figure 3(b) shows the normalized conductance measurements for a ZnO QD film measured in succinonitrile at 60 °C and on a dry film (the original traces are in supplementary material, Fig. S10). A few different measurements were performed on dry films, that is, when the film is not in the solution. First, conductance measurements were performed on the film directly after it was taken out of the solvent. Second, to minimize the amount of solvent around the film, the film was either blotted by a filter paper or placed under a vacuum for 1 min. Third, to ensure that the succinonitrile is completely solid, the film was plunged into THF at −80 °C for 10 s before the measurement (the conductance was measured at room temperature), and finally, the conductance was measured when the film was under vacuum. The vacuum measurements were performed by placing the sample in a metal tube with electrical feedthroughs, which was connected to a Varian TriScroll vacuum pump.

By comparing Figs. 3(a) and 3(b), it is clear that the charge stability of dry ZnO QD films is a lot better when succinonitrile is used. We attribute this to much reduced impurity diffusion in the solid succinonitrile that covers the film. In Fig. 3(b), dry films show much improved stability compared to the one in liquid succinonitrile at 60 °C. Figure S11 of the supplementary material shows a zoomed-in view of the dry films to highlight the differences between them. Of the dry films, the film that was simply taken out of the cell ("dry film," green line) shows the quickest drop in conductance. By decreasing the amount of succinonitrile (and consequently the total amount of solvent impurities) by either blotting or placing the film under vacuum for 1 min, the charge density becomes more stable. The stability increases even further by plunging the film in THF at −80 °C for a short time, allowing the solidification of succinonitrile to occur faster. The best results are obtained when measuring the ZnO QD film with a solid succinonitrile layer around it in vacuum. After a 2 h measurement, the conductance has decreased by about 4%. Apparently, even if a solid layer is around the ZnO QD film, and the whole sample is in vacuum, the conductance is not completely stable. It might be that succinonitrile is not solid in the nanopores of the QD film[32] or that internal electrochemical reactions of the ZnO QDs are taking place.[36] Despite the remaining slow decay of the conductance, the doping stability of ZnO QDs is enhanced enormously in solid succinonitrile.

CONCLUSIONS

In summary, we have shown by measuring ZnO QD films of different thicknesses that the instability of the charge density in electrochemically doped ZnO QDs films is predominantly due to oxidation by solvent impurities, even under very stringent air and water free conditions. We used two different methods to decrease the influence of solvent impurities on the doping stability. The first one includes reducing the solvent impurities, either electrochemically or chemically, while the second one employs a solid layer

covering the ZnO QD film. Using a cathodic preconditioning of the electrolyte solution, we obtained an 18-fold increase of the doping stability. However, after waiting several hours, the stability returned to its original value. Addition of superhydride Li[Et_3BH] results in a 100-fold increase in the doping stability. Furthermore, by reducing the solvent impurities, the CVs became more reversible. The largest increase in doping stability was obtained by removing the film, after charging it, from a warm succinonitrile solution. The succinonitrile solidifies and forms a solid protective layer around the sample that prevents impurity diffusion. In the best case, the charge density decreased by only 4% over the duration of 2 h.

SUPPLEMENTARY MATERIAL

See Supplementary material for a home-built interdigitated gold electrode, 2D differential absorbance spectra, differential absorbance during Fermi-level stability measurements, CVs of ZnO QDs measured in air, CVs of ZnO QD films of different thicknesses, profilometry results, cathodic preconditioning, the open circuit potential of the ZnO QD film by the addition of superhydride, CVs measured with different concentrations of Li[Et_3BH], non-normalized conductance measurements, CV of a ZnO QD film in succinonitrile, and a magnified conductance measurement.

ACKNOWLEDGMENTS

The authors acknowledge European research council horizon 2020 ERC, Grant Agreement No. 678004 (Doping on Demand).

REFERENCES

[1] S. C. Boehme, J. M. Azpiroz, Y. V. Aulin, F. C. Grozema, D. Vanmaekelbergh, L. D. Siebbeles, I. Infante, and A. J. Houtepen, Nano Lett. **15**(5), 3056–3066 (2015).
[2] P. Guyot-Sionnest, Microchim. Acta **160**(3), 309–314 (2008).
[3] P. Hoyer, R. Eichberger, and H. Weller, Ber. Bunsenges. Phys. Chem **97**, 630–635 (1993).
[4] S. C. Boehme, D. Vanmaekelbergh, W. H. Evers, L. D. A. Siebbeles, and A. J. Houtepen, J. Phys. Chem. C **120**(9), 5164–5173 (2016).
[5] W. van der Stam, S. Gudjonsdottir, W. H. Evers, and A. J. Houtepen, J. Am. Chem. Soc. **139**(37), 13208–13217 (2017).
[6] W. van der Stam, M. de Graaf, S. Gudjonsdottir, J. J. Geuchies, J. J. Dijkema, N. Kirkwood, W. H. Evers, A. Longo, and A. J. Houtepen, ACS Nano **12**(11), 11244–11253 (2018).
[7] L. Echegoyen and L. E. Echegoyen, Acc. Chem. Res. **31**, 593–601 (1998).
[8] M. L. Braunger, A. Barros, M. Ferreira, and C. A. Olivati, Electrochim. Acta **165**, 1 (2015).
[9] M. Shim, C. Wang, D. J. Norris, and P. Guyot-Sionnest, MRS Bull. **26**(12), 1005–1008 (2001).
[10] Q. Pei, G. Yu, C. Zhang, Y. Yang, and A. J. Heeger, Science **269**, 1086–1088 (1995).
[11] P. Matyba, K. Maturova, M. Kemerink, N. D. Robinson, and L. Edman, Nat. Mater. **8**(8), 672–676 (2009).
[12] Q. Pei, Y. Yang, G. Yu, C. Zhang, and A. J. Heeger, J. Am. Chem. Soc. **118**(16), 3922–3929 (1996).
[13] D. Yu, C. Wang, B. L. Wehrenberg, and P. Guyot-Sionnest, Phys. Rev. Lett. **92**(21), 216802 (2004).
[14] A. J. Houtepen, D. Kockmann and D. Vanmaekelbergh, Nano Lett. **8**(10), 3516–3520 (2008).
[15] S. C. Boehme, H. Wang, L. D. A. Siebbeles, D. Vanmaekelbergh, and A. J. Houtepen, ACS Nano **7**(3), 2500–2508 (2013).
[16] C. Jehoulet and A. J. Bard, J. Am. Chem. Soc. **113**, 5457–5459 (1991).
[17] J. J. Gooding, Electrochim. Acta **50**(15), 3049–3060 (2005).
[18] J. Gao, G. Yu, and A. J. Heeger, Appl. Phys. Lett. **71**(10), 1293–1295 (1997).
[19] A. K. Gooding, D. E. Gómez, and P. Mulvaney, ACS Nano **2**(4), 669–676 (2008).
[20] W. van der Stam, I. du Fosse, G. Grimaldi, J. O. V. Monchen, N. Kirkwood, and A. J. Houtepen, Chem. Mater. **30**(21), 8052–8061 (2018).
[21] J. Gao, Y. Li, G. Yu, and A. J. Heeger, J. Appl. Phys. **86**(8), 4594–4599 (1999).
[22] J. Niu, B. E. Conway, and W. G. Pell, J. Power Sources **135**(1-2), 332–343 (2004).
[23] I. E. Jacobs and A. J. Moule, Adv. Mater. **29**(42), 1703063 (2017).
[24] G. Lakhwani, R. F. H. Roijmans, A. J. Kronemeijer, J. Gilot, R. A. J. Janssen, and S. C. J. Meskers, J. Phys. Chem. C **114**, 14804–14810 (2010).
[25] A. M. Schimpf, C. E. Gunthardt, J. D. Rinehart, J. M. Mayer, and D. R. Gamelin, J. Am. Chem. Soc. **135**(44), 16569–16577 (2013).
[26] J. D. Rinehart, A. M. Schimpf, A. L. Weaver, A. W. Cohn, and D. R. Gamelin, J. Am. Chem. Soc. **135**(50), 18782–18785 (2013).
[27] L. E. Barrosse-Antle, A. M. Bond, R. G. Compton, A. M. O'Mahony, E. I. Rogers, and D. S. Silvester, Chem. - Asian J. **5**(2), 202–230 (2010).
[28] J. F. Coetzee, *Recommended Methods for Purification of Solvents and Tests for Impurities* (Pergamon Press, Great Britain, 1982).
[29] C. G. Zoski, *Handbook of Electrochemistry*, 1st ed. (Elsevier B.V., Netherlands, 2007).
[30] S. Gudjonsdottir, W. van der Stam, N. Kirkwood, W. H. Evers, and A. J. Houtepen, J. Am. Chem. Soc. **140**(21), 6582–6590 (2018).
[31] E. A. Meulenkamp, J. Phys. Chem. B **102**(29), 5566–5572 (1998).
[32] S. Gudjonsdottir, W. van der Stam, C. Koopman, B. Kwakkenbos, W. H. Evers, and A. J. Houtepen, ACS Appl. Nano Mater. **2**, 4900 (2019).
[33] J. Zhao, M. A. Holmes, and F. E. Osterloh, ACS Nano **7**(5), 4316–4325 (2013).
[34] E. Y. Tsui, G. M. Carroll, B. Miller, A. Marchioro, and D. R. Gamelin, Chem. Mater. **29**(8), 3754–3762 (2017).
[35] E. Y. Tsui, K. H. Hartstein, and D. R. Gamelin, J. Am. Chem. Soc. **138**(35), 11105–11108 (2016).
[36] I. du Fossé, S. ten Brinck, I. Infante, and A. J. Houtepen, Chem. Mater. **31**, 4575 (2019).
[37] K. Wu, J. Lim, and V. I. Klimov, ACS Nano **11**(8), 8437–8447 (2017).
[38] H. C. Brown, S. C. Kim, and S. Krishnamurthy, J. Org. Chem. **45**(1), 1–12 (1980).
[39] A. J. Bard and L. R. Faulkner, *Electrochemical Methods: Fundamentals and Applications*, 2nd ed. (John Wiley & Sons, New York, United States of America, 2001).